

# Characterization of Anomalous Diffusion from MR Signal may be a New Probe to Tissue Microstructure

Evren Özarslan, Peter J. Basser, Timothy M. Shepherd, Peter E. Thelwall,  
Baba C. Vemuri and Stephen J. Blackband

**Abstract**—Observation of translational self-diffusion of water molecules using magnetic resonance (MR) techniques has proven to be a powerful means to probe tissue microstructure. The collected MR signal depends on experimentally controllable parameters as well as the descriptors of tissue geometry. In order to obtain the latter, one needs to employ accurate models to characterize the dependence of the signal on the varied experimental parameters. In this work, a simple model describing diffusion in disordered media and fractal spaces is shown to describe the diffusion-time dependence of the diffusion attenuated MR signal obtained from biological specimens successfully. The model enables one to quantify the evolution of the average water displacement probabilities in terms of two exponents— $d_w$  and  $d_s$ . The experiments performed on excised human neural tissue samples and human red blood cell ghosts indicate that these two parameters are sensitive to tissue microstructure. Therefore, it may be possible to use the proposed scheme to generate novel contrast mechanism for classifying and segmenting tissue.

## I. INTRODUCTION

Nuclear magnetic resonance (NMR) provides a powerful framework to observe diffusion noninvasively. A moving particle in the presence of magnetic field inhomogeneities experiences different magnetic fields at different positions giving rise to local phase variations. As a result, the overall state of the magnetization is dependent upon motional history of the molecules. It has been observed from the early days of NMR that the effect of diffusion is easily detectable in liquid state by the NMR spectrometer [3]. This is because the timeframe in which the NMR signal is produced is typically sufficient for the molecules to travel a large enough distance in the presence of relatively small field gradients. Moreover, the resultant signal is dependent on the parameters such as diffusion time and diffusion gradient strength which can be controlled and modified during the experiment.

A significant advance has been the invention of the pulsed field gradient (PFG) experiments [13] that utilize a pair of spatially linear diffusion gradient pulses. The signal

This work was supported by the Intramural Research Program of NICHD, National Institutes of Health Grants R01-NS42075, R01-NS36992 and P41-RR16105, and the National High Magnetic Field Laboratory (NHMFL), Tallahassee.

E. Özarslan and Peter J. Basser are with the Section on Tissue Biophysics and Biomimetics, LIMB, NICHD, National Institutes of Health, Bethesda, MD 20892, USA. Correspondence address: [evren@helix.nih.gov](mailto:evren@helix.nih.gov)

T. M. Shepherd and Stephen J. Blackband are with the Department of Neuroscience, University of Florida, Gainesville, FL, USA.

P. E. Thelwall is with the Newcastle Magnetic Resonance Centre, University of Newcastle, Newcastle upon Tyne, UK.

B. C. Vemuri is with the Department of Computer and Information Science and Engineering, University of Florida, Gainesville, FL, USA.

attenuation values obtained by varying the magnitude of the gradient pulses, can be transformed into the water displacement probabilities. Moreover, by varying the diffusion gradient pulse separation, it is possible to observe diffusion occurring in different diffusion times. This makes it possible to probe different length scales using essentially the same experimental procedure.

MR measurements of molecular diffusion of water in neural tissue have found widespread use in biophysical as well as clinical investigations since it was shown that ischemic strokes can be detected much earlier with diffusion-weighted images when compared to traditional  $T_1$  and  $T_2$ -weighted images [8]. Although the sensitivity of diffusion-weighted acquisitions has been well-established, most studies have focused on the dependence of the MR signal on the diffusion gradient strength. However, it is possible to infer additional information by varying the other parameters of the experiment, such as the diffusion time.

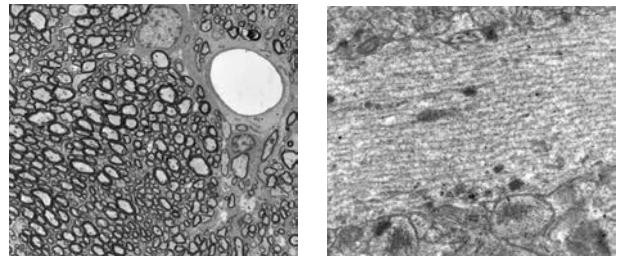


Fig. 1. Transmission electron microscopic images from axonal cells at different resolutions. The water molecules encounter different barriers at different length scales. The left panel shows a transverse view of axons, whereas the panel on the right depicts the longitudinal view of the intraaxonal space.

The neural tissue is well-known to have a very complicated architecture. However, neural tissue has traditionally been modeled to be composed of separate independent unrestricted compartments [9] or relatively simple geometric constructs [12] (such as cylinders, spheres, . . . etc.). However, in neural tissue, water molecules are expected to be restricted at different length scales by macromolecules, cytoskeleton, cell membranes and myelin (see Figure 1). Similarly, particles undergoing Brownian motion in disordered media and fractal spaces are restricted in all length scales giving rise to a nonlinear dependence of the mean square displacements on the diffusion-time—a process referred to as “anomalous diffusion” [2]. Therefore, a natural question to ask is whether the diffusion process within the neural tissue is

anomalous [10].

In this paper, we demonstrate that the diffusion-time dependence of the average propagators can be established using two power-laws. The scaling exponents have well-defined meanings in the context of diffusion taking place in fractal spaces. We demonstrate our results on data obtained from excised human gray-matter samples as well as human erythrocyte ghosts. The results indicate that the scaling exponents can be novel markers of tissue microstructure.

## II. THEORY

A diffusion process is considered normal, when the mean square displacement (MSD) of the diffusing particles has a linear diffusion-time dependence, i.e.,  $d_w = 2$  in the more general relationship

$$\text{MSD} = \langle r^2 \rangle \propto t^{2/d_w}. \quad (1)$$

Anomalous diffusion (the case when  $d_w \neq 2$ ) can be subgrouped according to the value of the scaling exponent. The case  $d_w > 2$  is called subdiffusion whereas the opposite case ( $d_w < 2$ ) describes a superdiffusive process. In the context of fractals, the scalar  $d_w$ , called the walk (or path or trail) dimension, is the fractal dimension of the trajectories followed by the particles undergoing random motion in a fractal space [2].

The spectral (fracton) dimension,  $d_s$ , is another scaling exponent that complements  $d_w$  in describing the scaling characteristics of the environments exhibiting fractal behavior. When diffusion is concerned, the return-to-origin-probability (RTOP) [4] for diffusing particles obeys the power-law relationship [2]

$$\text{RTOP} = P(r=0, t) \propto t^{-d_s/2}, \quad (2)$$

where  $P(r, t)$  is the probability that particles move a distance  $r$  in time  $t$ .

In fractal environments,  $d_w$  and  $d_s$  are sufficient to determine the fractal dimension  $d_f$ , which characterizes the scaling of mass density with different length scales. The relationship between these three exponents is simply

$$d_f = \frac{d_w d_s}{2}. \quad (3)$$

These scaling relationships can be incorporated into a particular form for the diffusion propagator. For example, the isotropic propagator in a fractal space embedded in dimension  $d$  is expected to be of the form

$$P(r, t) \propto \frac{r^{d_f-d}}{t^{d_s/2}} \Phi\left(\frac{r}{t^{1/d_w}}\right). \quad (4)$$

Here, the scaling relation given in Eq. 1 is ensured by the argument of the function  $\Phi$ . The numerator  $r^{d_f-d}$  has to do with the scaling of the ‘‘mass’’ of the fractal with distance and the denominator  $t^{d_s/2}$  is necessary for the normalization condition.

PFG MR experiments can be performed conveniently by applying gradients with different strengths while keeping the gradient direction fixed. In this case, an ensemble averaged

water displacement probability function  $\bar{P}_1(z, \Delta)$  can be computed by taking the Fourier transform of the MR signal attenuations, i.e.

$$\bar{P}_1(z, \Delta) = \int_{-\infty}^{\infty} E(q, \Delta) e^{-2\pi i q z} dq. \quad (5)$$

Note that the Fourier slice theorem implies that  $\bar{P}_1(z, \Delta)$  is just the projection of the three-dimensional propagator on the  $z$ -axis, which is defined by the orientation of the applied diffusion sensitizing gradients. In the above expression  $\Delta$  is the duration between the application of the two diffusion gradient pulses and  $q = \gamma \delta G / 2\pi$ , where  $\gamma$  is the gyromagnetic ratio,  $\delta$  is the diffusion pulse duration assumed to be much smaller than  $\Delta$ , and  $G$  is the magnitude of the diffusion gradient.

Note that in isotropic space, the following expression holds:

$$\langle r^2 \rangle = \langle x^2 + y^2 + z^2 \rangle = 3\langle z^2 \rangle. \quad (6)$$

Therefore,  $\langle r^2 \rangle$  and  $\langle z^2 \rangle$  have the same scaling relationship characterized by the same exponent  $2/d_w$ . Consequently, in the estimation of  $d_w$ , one can use the straightforward relationship

$$\langle z^2 \rangle = -\frac{1}{2\pi^2} \lim_{q \rightarrow 0} \frac{\partial \log E(q, \Delta)}{\partial q^2} = 2D(\Delta) \Delta, \quad (7)$$

where  $D(\Delta)$  is a diffusion-time dependent diffusion coefficient [11].

In analogy with Eq. 2, we expect the scaling behavior of the projected (one-dimensional) propagator at the  $z = 0$  value to be of the form

$$\bar{P}_1(z=0, \Delta) = \int_{-\infty}^{\infty} E(q, \Delta) dq, \quad (8)$$

$$\propto \Delta^{-d'_s/2}. \quad (9)$$

Note that there is no simple relationship between  $d_s$  and  $d'_s$  even in the case of isotropic space.

A reasonable form for the projected propagator that satisfies all the desired scaling properties is given by

$$P_1(z, \Delta) \propto \frac{z^{d'_f-1}}{\Delta^{d'_s/2}} \Psi\left(\frac{z}{\Delta^{1/d_w}}\right). \quad (10)$$

where  $d'_f$  is defined as  $d'_f = d_w d'_s / 2$ .

Finally, the true spectral dimension can be estimated in isotropic space using Eq. 2 since it is possible to compute the RTOP values through the relationship

$$\text{RTOP} = 4\pi \int_0^{\infty} E(q, \Delta) q^2 dq, \quad (11)$$

which is just the  $r = 0$  value of the three-dimensional Fourier transform of the isotropic signal attenuation function.

## III. METHODS

In this work, we present experimental results obtained from  $q$ -space spectroscopy experiments performed on three different samples. One of the samples was a human erythrocyte ghost prepared as described in [14]. These ghosts serve as a system that is expected to exhibit normal diffusion as

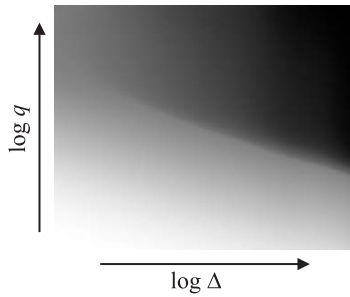


Fig. 2. The entire data set from the tumor sample. The grayscale intensity represents the MR signal attenuation  $E(q, \Delta)$  after interpolation and histogram equalization (for display purposes only).

there are restrictions to diffusion only at one length scale due to the cellular membranes. The other two samples were a human cerebral cortex tissue from a normal person and a human glioblastoma multiforme (or grade-4 astrocytoma) tumor. The experiments were performed using a 14.1T (600 MHz) Bruker Avance spectrometer and a gradient coil system that is capable of producing 3 T/m gradients along each of the three orthogonal directions. Because it was necessary to perform some of the measurements at longer diffusion times, a diffusion-weighted stimulated echo pulse sequence was used. The experimental parameters for the erythrocyte ghosts and the tissue samples were slightly different because of the rapid signal attenuation in the ghosts. The spectroscopy data from the brain samples were acquired with TE/TR values of 11ms/4s. The gradient pulse duration ( $\delta$ ) was 2.4ms, and the  $q$ -space measurements were repeated 12 times varying the gradient pulse separation ( $\Delta$ ) between 12 and 613ms on a logarithmic scale. For each diffusion time, a total of 129  $q$ -values were used, with gradient strengths of up to 4892.5 mT/m. The  $q$ -space resolution was  $2\mu\text{m}$ . The acquisition protocol for the erythrocyte ghost samples had the identical parameters except the following modifications: TR was set to 5s, the maximum gradient strength used was 4194mT/m and  $\delta$  was 2ms, so that the  $q$ -space resolution was  $2.8\mu\text{m}$ . The  $q$ -axis was sampled on 65 points. Figure 2 depicts an “image” of the entire data set ( $E(q, \Delta)$  values) acquired from the tumor sample.

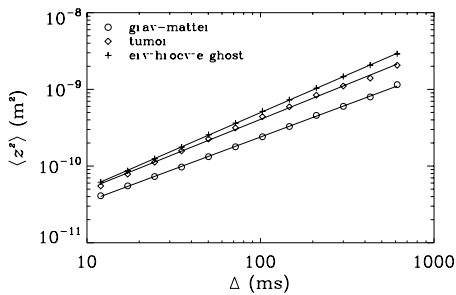


Fig. 3. Mean square displacements obtained from different diffusion times. The linear behavior in this double logarithmic plot indicates a power-law relationship.

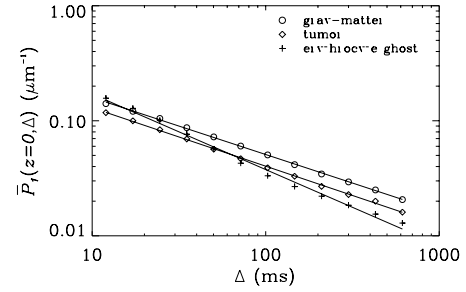


Fig. 4. The probabilities for water molecules to return to the  $xy$ -plane with varying diffusion-times. The slopes of the fitted lines yield the scaling exponent  $d'_s$ .

#### IV. RESULTS

Figure 3 shows the dependence of the mean square displacements on diffusion time. In this figure, the  $\langle z^2 \rangle$  values were estimated using a two point difference of the logarithm of the signal value near the origin as implied by Eq. 7. The expected power-law behavior was evident and the fits obtained were almost perfect with correlation coefficients above 0.999. The estimated  $d_w$  values were  $2.036 \pm 0.005$ ,  $2.371 \pm 0.014$  and  $2.189 \pm 0.029$  for the erythrocyte ghost, normal gray matter and tumor tissue respectively. These results indicate that diffusion in neural tissue is in the subdiffusive regime whereas in the red blood cell ghosts it was very close to normal as expected.

Figure 4 shows the diffusion-time dependence of the probability of particles to move to the  $xy$ -plane. The slopes of the fitted lines yield the scaling exponents  $d'_s$  for all samples as implied by Eq. 8. The fits were very satisfactory for all three samples justifying the speculated power-law. The estimated  $d'_s$  values were  $1.312 \pm 0.036$ ,  $0.991 \pm 0.008$  and  $1.018 \pm 0.009$  for the erythrocyte ghost, normal gray matter and tumor tissue respectively.

Figure 5 depicts the diffusion-time dependence of the RTOP values estimated by integrating the signal attenuation values with the measure  $q^2 dq$  consistent with Eq. 11. The slope of the fitted lines are used in estimating the scaling exponents  $d_s$ . Since the values at high  $q$ -values contribute

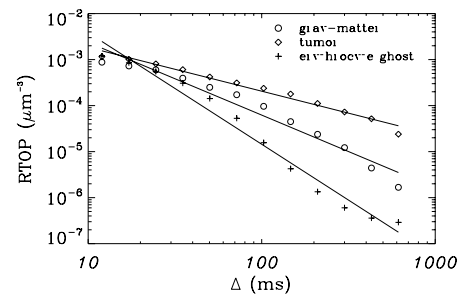


Fig. 5. The return-to-the-origin probabilities as a function of diffusion times. The slopes of the fitted lines yield the scaling exponent  $d_s$ .

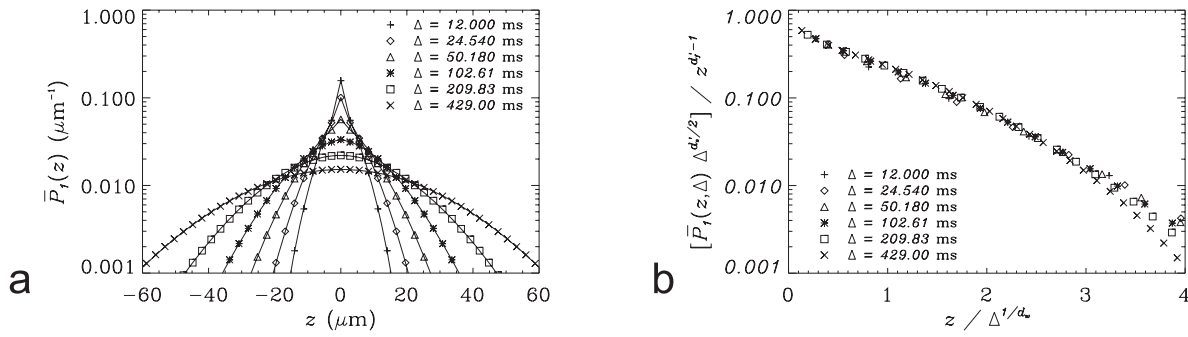


Fig. 6. **a.** Ensemble averaged diffusion propagators obtained by Fourier transforming the signal attenuation values from the erythrocyte ghost sample. **b.** The part of the same propagators with positive  $z$  values, displayed by incorporating the estimated scaling relations.

more significantly to the RTOP values, it is a more difficult task to evaluate the integrals and hence the  $d_s$  values. Consequently, there was some reduction in the quality of the fits obtained. However, the correlation coefficients were still larger than 0.97. The estimated  $d_s$  values were  $4.852 \pm 0.233$ ,  $3.166 \pm 0.210$  and  $1.909 \pm 0.091$  for the erythrocyte ghost, normal gray matter and tumor tissue respectively.

As demonstrated in the theory section, the quantified scaling exponents are consistent with the diffusion propagator to be of the form given in Eq. 10. Note that according to this relation plots of  $P_1(z, \Delta) \Delta^{d_s/2} / z^{d_s-1}$  vs.  $z \Delta^{-1/d_w}$  are expected to yield identical curves for propagators with different diffusion times. Figure 6a shows the propagators with different diffusion times computed from the erythrocyte ghost sample. The probability values for the positive  $z$ -axis used in this plot are replotted in figure 6b to show the shape of the function  $\Psi(x)$ . Although small deviations at long diffusion times were visible, the collapse of the data points from different diffusion-times on to the same curve is clear. Every other time points were excluded in both plots for clarity.

## V. DISCUSSION AND CONCLUSION

There have been several theoretical attempts to relate the walk dimension directly to the signal acquired via PFG experiments [1], [5], [7], [6], [15]. Although these approaches may be preferable as they include the effects of finite pulse widths, they don't provide a direct estimation strategy for the other exponents such as the spectral dimension.

In order to characterize the diffusion-time dependence of the MR signal, the description for diffusion in fractal spaces and disordered media was used. The experiments performed on samples with different expected diffusional characteristics indicate that the model is quite accurate in all cases and may be employed in biophysical as well as clinical investigations in the future. The quantified scaling exponents may provide a new contrast mechanism which may improve the diagnostic utility and specificity of diffusion MR.

## REFERENCES

- [1] J. R. Banavar, M. Lipsicas, and J. F. Willemsen, "Determination of the random-walk dimension of fractals by means of NMR," *Phys Rev B*, vol. 32, no. 9, p. 6066, 1985.
- [2] D. ben-Avraham and S. Havlin, *Diffusion and Reactions in Fractals and Disordered Systems*. Cambridge, UK: Cambridge University Press, 2000.
- [3] E. L. Hahn, "Spin echoes," *Phys Rev*, vol. 80, pp. 580–594, 1950.
- [4] M. D. Hürlimann, L. M. Schwartz, and P. N. Sen, "Probability of return to origin at short times: A probe of microstructure in porous media," *Phys Rev B*, vol. 51, no. 21, pp. 14 936–14 940, 1995.
- [5] G. Jug, "Theory of NMR field-gradient spectroscopy for anomalous diffusion in fractal networks," *Chem Phys Lett*, vol. 131, no. 1,2, pp. 94–97, 1986.
- [6] J. Kärgler, H. Pfeifer, and G. Vojta, "Time correlation during anomalous diffusion in fractal systems and signal attenuation in NMR field-gradient spectroscopy," *Phys Rev A*, vol. 37, no. 11, pp. 4514–4517, 1988.
- [7] J. Kärgler and G. Vojta, "On the use of NMR pulsed field-gradient spectroscopy for the study of anomalous diffusion in fractal networks," *Chem Phys Lett*, vol. 141, no. 5, pp. 411–413, 1987.
- [8] M. E. Moseley, Y. Cohen, J. Mintorovitch, L. Chileuitt, H. Shimizu, J. Kucharczyk, M. F. Wendland, and P. R. Weinstein, "Early detection of regional cerebral ischemia in cats: comparison of diffusion and  $T_2$ -weighted MRI and spectroscopy," *Magn Reson Med*, vol. 14, pp. 330–346, 1990.
- [9] T. Niendorf, R. M. Dijkhuizen, D. G. Norris, M. van Lookeren Campagne, and K. Nicolay, "Biexponential diffusion attenuation in various states of brain tissue: implications for diffusion-weighted imaging," *Magn Reson Med*, vol. 36, no. 6, pp. 847–857, 1996.
- [10] E. Özarslan, P. J. Basser, B. C. Vemuri, T. M. Shepherd, P. E. Thelwall, and S. J. Blackband, "Observation of anomalous diffusion in excised tissue using the diffusion time dependence of the MR signal," in *47<sup>th</sup> Experimental Nuclear Magnetic Resonance Conference*, 2006.
- [11] P. N. Sen, "Time-dependent diffusion coefficient as a probe of geometry," *Concept Magn Reson A*, vol. 23A, no. 1, pp. 1–21, 2004.
- [12] G. J. Stanis, A. Szafer, G. A. Wright, and R. M. Henkelman, "An analytical model of restricted diffusion in bovine optic nerve," *Magn Reson Med*, vol. 37, no. 1, pp. 103–111, 1997.
- [13] E. O. Stejskal and J. E. Tanner, "Spin diffusion measurements: Spin echoes in the presence of a time-dependent field gradient," *J Chem Phys*, vol. 42, no. 1, pp. 288–292, 1965.
- [14] P. E. Thelwall, S. C. Grant, G. J. Stanis, and S. J. Blackband, "Human erythrocyte ghosts: Exploring the origins of multiexponential water diffusion in a model biological tissue with magnetic resonance," *Magn Reson Med*, vol. 48, no. 4, pp. 649–657, 2002.
- [15] A. Widom and H. J. Chen, "Fractal Brownian motion and nuclear spin echoes," *J Phys A*, vol. 28, pp. 1243–1247, 1995.